ELSEVIER

J. Non-Newtonian Fluid Mech. 135 (2006) 109–116

Journal of Non-Newtonian Fluid Mechanics

www.elsevier.com/locate/jnnfm

Accurate asymptotic formulas for the transient PDF of a FENE dumbbell in suddenly started uniaxial extension followed by relaxation

Ludwig C. Nitsche*

Department of Chemical Engineering, University of Illinois at Chicago, 810 South Clinton Street, Chicago, IL 60607, USA

Received 22 June 2005; received in revised form 26 December 2005; accepted 3 January 2006

Abstract

Singular perturbation theory is combined with the method of multiple scales to derive an asymptotic solution for the transient, one-dimensional probability density function (PDF) of a FENE dumbbell in a suddenly started uniaxial extensional flow. We consider the dual asymptotic limit of large dimensionless spring length, $L = \epsilon^{-1}$, and large dimensionless elongation rate (or Weissenberg number), $\Gamma = \gamma/\epsilon$, with these two quantities remaining in a fixed (arbitrary) proportion, γ. The analytical formula for the transient PDF agrees closely with numerics in both (i) the central, approximately Gaussian core, and (ii) a thin boundary layer near the limit of extension [see, e.g., R. Keunings, J. Non-Newtonian Fluid Mech. 68 (1997) 85–100]. Stress buildup and stress–extension curves are well predicted. We also explain the collapse of different dumbbell lengths onto a single stress–extension line, $\tau = 2\Gamma\langle x^2\rangle$, which has been observed numerically in connection with transient stress-birefringence [P.S. Doyle, E.S.G. Shaqfeh, G.H. McKinley, S.H. Spiegelberg, J. Non-Newtonian Fluid Mech. 76 (1998) 79–110]. This result agrees with the large-strain plateau in the transient stress-optic coefficient for large Weissenberg number [R. Sizaire, G. Lielens, I. Jaumain, R. Keunings, V. Legat, J. Non-Newtonian Fluid Mech. 82 (1999) 233–253]. For relaxation of the FENE dumbbell from its fully stretched configuration, a Gaussian approximation of the PDF—whose time-dependent position and width are given by closed analytical formulas—matches the numerical results extremely well. The slope of the advective velocity is interpreted as a negative contribution to the effective diffusion coefficient. The asymptotic theory supports the recently proposed L closure [G. Lielens, P. Halin, I. Jaumain, R. Keunings, V. Legat, J. Non-Newtonian Fluid Mech. 76 (1998) 249–279].

Keywords: FENE dumbbell; Dilute polymer solution; Transient rheology; Stress-optic coefficient; Singular perturbation theory; Multiple scale analysis

1. Introduction

In the transient rheology of dilute polymer solutions, the behavior of a finitely extensible nonlinearly elastic (FENE) dumbbell immersed in a suddenly started, uniaxial extensional flow represents a long-standing and ubiquitous problem [2,10,24,25], which is often compared with more complicated models of polymers [5–7,21,29,31]. The conformational state of the dumbbell at any time is described in statistical terms by a distribution of probability density over all possible end-to-end vectors (length and orientation). Macroscopic rheological properties can be calculated as integrals of the probability density function (PDF). The stretching mode emerges as the most important degree of freedom in elongational flow [10,11,22], and the associated one-dimensional PDF, $P(x, \hat{t})$, is governed by a standard (dimensionless) Smoluchowski equation, which balances local accumulation of probability at each length x with fluxes due to the (nonlinear) connecting spring, hydrodyamic drag on the beads, and Brownian motion [2,10,24,25].

$$\frac{\partial P}{\partial \hat{t}} + \frac{\partial}{\partial x}\left\{\left(\Gamma - \frac{1}{2}\frac{1}{1 - x^2/L^2}\right)xP - \frac{1}{2}\frac{\partial P}{\partial x}\right\} = 0, \quad 0 < x < L \tag{1}$$

with L the dimensionless limit of extension. Typically the finite extensibility parameter L^2 can range from 50 to over 4000 [6,8,10,21], which makes $L \to \infty$ a physically realistic asymptotic limit. The dimensionless elongation rate Γ is equivalent to a Weissenberg number.

Because Eq. (1) has, as yet, eluded analytical solution, an extensive literature has grown around averaging and closure schemes, which proceed from reasonable (but mathematically ad hoc) simplified assumed shapes for the PDF, to reduce the Smoluchowski equation to one or more ODEs governing the time dependence of the relevant shape parameters. Most common has been the Gaussian shape [16,18,26,28,32], whose

* Tel.: +1 312 996 3469; fax: +1 312 996 0808.
E-mail address: lcn@uic.edu (L.C. Nitsche).

0377-0257/$ – see front matter © 2006 Elsevier B.V. All rights reserved.
doi:10.1016/j.jnnfm.2006.01.008

qualitative limitations were recently remedied by the box-spike shape of the L closure [11,12]. Numerical solutions provide valuable insight and a quantitative test for such approximations; stochastic simulations have emerged as the most prominent computational method for this problem [8,10–12,17].

The availability of numerically calculated PDFs does not diminish the desirability of an analytical solution to Eq. (1), because the latter would offer mechanistic *explanations* for the observed behavior in concise mathematical language, and would also make accurate calculations for an important class of FENE problems much easier and very quick on a personal computer.

This paper presents an asymptotic solution, based upon the method of singular perturbations, which compares very favorably with numerical results—even for moderate values of L. Our derivation also provides a rigorous theoretical basis for the L closure.

2. Overview of the asymptotic method

The asymptotic approach used here—singular perturbations combined with multiple timescales [1]—exploits key qualitative features of the behavior of the FENE dumbbell as it gets stretched by the elongational flow. These features were first elucidated numerically [10,11,21]. At the initial equilibrium, the PDF is a roughly Gaussian peak, which represents a balance between Brownian fluctuations tending to extend the dumbbell and the restoring force of the spring. A sufficiently strong elongational flow (here we will assume asymptotically large Γ) overpowers the linear regime of the spring at small extensions x, and pulls probability outward. The probability density in the central core (outer solution) eventually decays to zero *as if* the dumbbell were infinitely extensible. Whatever probability *would have* extended beyond $x = L$ at any time gets rearranged into a second, much thinner peak (inner solution) just short of $x = L$.

The asymptotic analysis of Nitsche et al. [15] for the FENE dumbbell *with variable friction* [4,6,9,19,20,23] applied to the limit $L \to \infty$. In combination with an ord(1) elongation rate Γ, the linear growth of the bead friction coefficient with extension was sufficient to compress the outwardly accumulating probability against the (soft) stop of the spring into an asymptotically thin boundary layer. Correspondingly, a separation of timescales emerged, whereby the boundary layer equilibrated to the incoming probability density much faster than the central peak drained off into the boundary layer.

For the FENE dumbbell with *fixed friction*, Eq. (1), the peak near the limit of extension is *not* asymptotically narrow as $L \to \infty$. Motivated by numerical observations along these lines, Lielens et al. [11] formulated an extended L closure, in which the terminal delta-function spike was widened into a rectangular box. Here we consider a dual asymptotic limit, in which Γ increases in proportion to L. This assumption recovers the boundary-layer character of the problem.

Aside from developing the asymptotic solution for a different dumbbell model (FENE with fixed friction versus FENE with variable friction), this paper goes beyond the analysis of Nitsche et al. [15] in two ways—to obtain quantitatively accurate PDFs at moderate values of L.

- Here the outer solution is derived through second order, whereas the previous paper did not involve the outer solution in detail.
- The inner solution is extended from the previous leading-order result to the first correction. In the process we expose the source of asymmetry in the boundary layer.

We define the small perturbation parameter $\epsilon = L^{-1}$, and consider an asymptotically large elongation rate $\Gamma = \gamma\epsilon^{-1}$. Recast in terms of a reduced time variable $t = \epsilon^{-1}\hat{t}$, Eq. (1) becomes

$$\frac{\partial P}{\partial t} + \frac{\partial}{\partial x}\left\{\left(\gamma - \frac{\epsilon}{2}\frac{1}{1-\epsilon^2x^2}\right)xP - \frac{\epsilon}{2}\frac{\partial P}{\partial x}\right\} = 0, \quad 0 < x < \epsilon^{-1} \tag{2}$$

3. Outer solution

The initial, equilibrium PDF is obtained by solving the steady-state version of Eq. (2) with $\gamma = 0$. The exact solution

$$P(x,0) = \left\{\int_0^{\epsilon^{-1}} \left(1-\epsilon^2x^2\right)^{1/(2\epsilon^2)}\,\mathrm{d}x\right\}^{-1}\left(1-\epsilon^2x^2\right)^{1/(2\epsilon^2)} \tag{3}$$

is actually less useful than the asymptotic formula

$$P(x,0) \sim \left(\frac{2}{\pi}\right)^{1/2}\exp\left(-\frac{x^2}{2}\right)\left[1+\epsilon^2\left(\frac{3}{4}-\frac{x^4}{4}\right)+\cdots\right] \tag{4}$$

that reveals the roughly Gaussian shape.

At first glance the nonlinear FENE factor in Eq. (2) seems to pose a serious difficulty—until one examines the characteristic curves (x versus t) associated with the advective portion of the flux,

$$\frac{\mathrm{d}x}{\mathrm{d}t} = v(x;\epsilon,\gamma) = \left(\gamma - \frac{\epsilon}{2}\frac{1}{1-\epsilon^2x^2}\right)x, \quad x(0) = x_0 \tag{5}$$

for which the exact solution is

$$t = \frac{1}{\gamma-\epsilon/2}\left\{\ln\left(\frac{x}{x_0}\right) - \frac{\epsilon}{4\gamma}\ln\left[\frac{2\gamma(1-\epsilon^2x^2)-\epsilon}{2\gamma(1-\epsilon^2x_0^2)-\epsilon}\right]\right\} \tag{6}$$

Even when ϵ is not very small, the only discernible effect of the FENE factor is to cause the characteristic curve to level off *very* abruptly at the terminal value

$$x^*(\epsilon,\gamma) = \epsilon^{-1}\sqrt{1-\frac{\epsilon}{2\gamma}} \tag{7}$$

at which v vanishes. One obtains essentially indistinguishable results by neglecting the FENE factor in the velocity,

$$\frac{\mathrm{d}x}{\mathrm{d}t} = \left(\gamma - \frac{\epsilon}{2}\right)x \tag{8}$$

and simply truncating the solution:

$$x(t) \approx \begin{cases} x_0\mathrm{e}^{(\gamma-\epsilon/2)t}, & t \le t^* \\ x^*, & t > t^* \end{cases} \qquad t^* = \frac{\ln(x^*/x_0)}{\gamma-\epsilon/2} \tag{9}$$

This observation commends using a much simpler Smoluchowski equation with a linear advective term

$$\frac{\partial P^{[O]}}{\partial t} + \frac{\partial}{\partial x}\left\{\left(\gamma - \frac{\epsilon}{2}\right) x P^{[O]} - \frac{\epsilon}{2}\frac{\partial P^{[O]}}{\partial x}\right\} = 0 \tag{10}$$

throughout the outer region $0 \le x < x^*(\epsilon, \gamma)$. The initial PDF from Eq. (4) suggests the regular perturbation expansion

$$P^{[O]}(x, t; \epsilon) = P_0^{[O]}(x, t; \epsilon) + \epsilon^2 P_2^{[O]}(x, t; \epsilon) + \cdots \tag{11}$$

where both of the functions $P_0^{[O]}(x, t; \epsilon)$ and $P_2^{[O]}(x, t; \epsilon)$ satisfy Eq. (10) with the respective initial conditions

$$P_0^{[O]}(x, 0; \epsilon) = \left(\frac{2}{\pi}\right)^{1/2} \exp\left(-\frac{x^2}{2}\right) \tag{12}$$

$$P_2^{[O]}(x, 0; \epsilon) = \left(\frac{2}{\pi}\right)^{1/2} \left(\frac{3}{4} - \frac{x^4}{4}\right) \exp\left(-\frac{x^2}{2}\right) \tag{13}$$

Eq. (10) is exactly solvable for a Gaussian initial PDF:

$$P_0^{[O]}(x, t; \epsilon) = \frac{1}{\ell(t)}\left(\frac{2}{\pi}\right)^{1/2} \exp\left\{-\frac{1}{2}\left[\frac{x}{\ell(t)}\right]^2\right\} \tag{14}$$

with

$$\ell(t) = \left\{\left(1 + \frac{\epsilon}{2\gamma - \epsilon}\right) e^{(2\gamma - \epsilon)t} - \frac{\epsilon}{2\gamma - \epsilon}\right\}^{1/2} \tag{15}$$

To solve for $P_2^{[O]}(x, t; \epsilon)$ we can neglect the diffusion term in Eq. (10), as this will contribute (i) at order ϵ while the peak is of ord(1) width, and (ii) even less as the peak widens. The resulting first-order PDE can be solved by the method of characteristics [3] to yield

$$P_2^{[O]}(x, t; \epsilon) \sim e^{-(\gamma - \epsilon/2)t} P_2^{[O]}\left(x e^{-(\gamma - \epsilon/2)t}, 0; \epsilon\right) \tag{16}$$

$$P_2^{[O]}(x, t; \epsilon) \sim \left(\frac{2}{\pi}\right)^{1/2} \left[\frac{3}{4} - \frac{1}{4}\left(x e^{-(\gamma - \epsilon/2)t}\right)^4\right] \times \exp\left[-\left(\gamma - \frac{\epsilon}{2}\right) t - \frac{1}{2}\left(x e^{-(\gamma - \epsilon/2)t}\right)^2\right] \tag{17}$$

In summary, the outer solution through second-order terms is given by Eqs. (11), (14), (15) and (17). As far as the boundary layer is concerned, the important quantity is the cumulative amount of probability A that accumulates beyond x^*.

$$A(t) \underset{=}{\text{def}} \int_{x^*}^{\infty} P^{[O]}(x, t)\, dx \tag{18}$$

$$A(t) \sim \text{erfc}\left[\frac{x^*}{\ell(t)\sqrt{2}}\right] - \frac{\epsilon^2}{4}\left(\frac{2}{\pi}\right)^{1/2} [X^*(t)]\left\{3 + [X^*(t)]^2\right\} \times \exp\left\{-\frac{1}{2}[X^*(t)]^2\right\} \tag{19}$$

with

$$X^*(t) = x^* e^{-(\gamma - \epsilon/2)t} \tag{20}$$

For the rate of change of accumulated probability we find

$$A'(t) \sim \left(\gamma - \frac{\epsilon}{2}\right) x^* P^{[O]}(x^*, t) + \frac{\epsilon}{\sqrt{2\pi}} \frac{x^*}{[\ell(t)]^3} \exp\left\{-\frac{1}{2}\left[\frac{x^*}{\ell(t)}\right]^2\right\} \tag{21}$$

The second term is the diffusive flux, which contributes at the same order as the ϵ portion of the advective flux from $P_2^{[O]}$.

4. Inner Solution

The boundary layer is centered at $x = x^*$, Eq. (7), where the advective velocity vanishes. Using the stretched inner coodinate

$$\eta = \epsilon^{-1}(x - x^*) \tag{22}$$

the Smoluchowski Eq. (2) can be written as follows:

$$\epsilon\frac{\partial P^{[I]}}{\partial t} + \frac{\partial}{\partial \eta}\left\{\left[V_0(\eta) + \epsilon V_1(\eta) + \epsilon^2 V_2(\eta) + \cdots\right] P^{[I]} - \frac{1}{2}\frac{\partial P^{[I]}}{\partial \eta}\right\} = 0 \tag{23}$$

with

$$V_0(\eta) = -4\gamma^2\eta \tag{24}$$

$$V_1(\eta) = 2\gamma\eta(1 - 8\gamma^2\eta) \tag{25}$$

$$V_2(\eta) = 2\gamma^2\eta^2(3 - 32\gamma^2\eta) \tag{26}$$

The ϵ factor multiplying the time derivative in Eq. (23) suggests that we should use the two-timescale expansion

$$P^{[I]}(\eta, t; \epsilon) \sim \epsilon^{-1} P_0^{[I]}(\eta, \tau, T) + P_1^{[I]}(\eta, \tau, T) + \cdots \tag{27}$$

with the fast and slow time variables

$$\tau = \epsilon^{-1} t, \quad T = t \tag{28}$$

The asymptotic expansion (27) begins at order ϵ^{-1} in order that the inner solution can accumulate ord(1) probability within a peak of ord(ϵ) width.

Substituting Eq. (27) into the inner Smoluchowski Eq. (23) yields a hierarchy of parabolic partial differential equations in η and τ, with the slow time variable T appearing as a parameter

$$\frac{\partial P_0^{[I]}}{\partial \tau} + \frac{\partial}{\partial \eta}\left[V_0(\eta) P_0^{[I]} - \frac{1}{2}\frac{\partial P_0^{[I]}}{\partial \eta}\right] = 0 \tag{29}$$

$$\frac{\partial P_1^{[I]}}{\partial \tau} + \frac{\partial}{\partial \eta}\left[V_0(\eta) P_1^{[I]} - \frac{1}{2}\frac{\partial P_1^{[I]}}{\partial \eta}\right] = -\frac{\partial P_0^{[I]}}{\partial T} - \frac{\partial}{\partial \eta}\left[V_1(\eta) P_0^{[I]}\right] \tag{30}$$

The two-timescale analysis of Nitsche et al. [15] shows how the boundary-layer solution equilibrates rapidly (on the fast timescale τ) to the influx of probability (on the slow timescale T) from the outer solution. These detailed considerations boil

down to the following simplified operational procedure. At each order one solves for the steady-state PDF that corresponds to the limit $\tau \to \infty$ in Eqs. (29) and (30). The free "constants" that arise (which are actually functions of the slow time parameter T) are determined by maintaining the total probability—integrated over the inner PDF—at the value $A(T)$ given by Eq. (19). At leading order we find

$$P_0^{[\mathrm{I}]}(\eta, T) = A(T)\left(\frac{2\gamma}{\sqrt{\pi}}\right)\mathrm{e}^{-(2\gamma\eta)^2} \tag{31}$$

To obtain quantitatively accurate results at moderate values of ϵ, we must carry the analysis one order farther than did the analogous work [15] on FENE dumbbells with variable friction. Solving the steady-state version of Eq. (30),

$$\frac{\mathrm{d}}{\mathrm{d}\eta}\left[V_0(\eta)P_1^{[\mathrm{I}]} - \frac{1}{2}\frac{\mathrm{d}P_1^{[\mathrm{I}]}}{\mathrm{d}\eta}\right] = -\left(\frac{2\gamma}{\sqrt{\pi}}\right)\left\{A'(T)\mathrm{e}^{-(2\gamma\eta)^2} + A(T)\frac{\mathrm{d}}{\mathrm{d}\eta}\left[V_1(\eta)\mathrm{e}^{-(2\gamma\eta)^2}\right]\right\} \tag{32}$$

we find the first correction to the inner PDF:

$$P_1^{[\mathrm{I}]}(\eta, T) = \frac{A(T)}{\sqrt{\pi}}\left[(2\gamma\eta)^2 - \frac{8\gamma}{3}(2\gamma\eta)^3 - \frac{1}{2}\right]\mathrm{e}^{-(2\gamma\eta)^2} + \frac{A'(T)}{\gamma}\left\{G(2\gamma\eta) - \frac{1}{\sqrt{\pi}}\left[1.4452 + \frac{1}{2}\ln\left(\frac{2\gamma x^*}{\epsilon}\right)\right]\mathrm{e}^{-(2\gamma\eta)^2}\right\} \tag{33}$$

Here the function G is given by

$$G(\alpha) = \mathrm{e}^{-\alpha^2}\int_\alpha^\infty F(\beta)\mathrm{e}^{\beta^2}\,\mathrm{d}\beta,$$

$$F(\beta) = \begin{cases} -\frac{1}{2}\mathrm{erfc}(-\beta) + 1, & \beta < 0 \\ \frac{1}{2}\mathrm{erfc}(\beta), & \beta \geq 0 \end{cases} \tag{34}$$

It is straightforward to interpolate function values $G(\alpha)$ from a look-up table generated by numerical quadrature of Eq. (34); see Fig. 1. We note the asymptotic behavior

$$G(\alpha) \sim -1/(2\alpha) \quad \text{as } \alpha \to -\infty \tag{35}$$

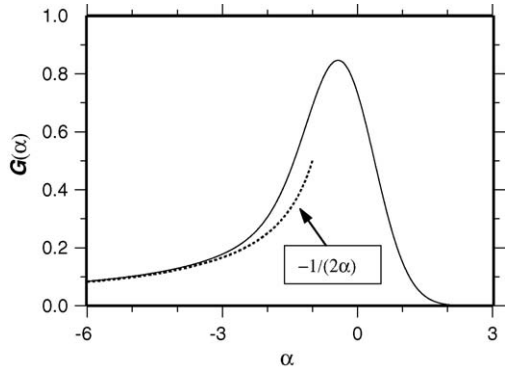

Fig. 1. The function $G(\alpha)$ defined in Eq. (34).

In deriving Eq. (33), we have chosen the constants of integration to (i) yield zero flux at the limit of extension, and (ii) prevent the first correction altering the total probability—which had already been set in the boundary layer at zeroth order:

$$0 = \int_0^1 P_1^{[\mathrm{I}]}\left(\frac{x - x^*}{\epsilon}, T\right)\mathrm{d}x = \epsilon\int_{-x^*/\epsilon}^\infty P_1^{[\mathrm{I}]}(\eta, T)\,\mathrm{d}\eta + \left\{\begin{array}{c}\text{Exponentially}\\ \text{small terms}\end{array}\right\} \tag{36}$$

Note the appearance of an $\mathrm{O}(\ln\epsilon)$ term, proportional to the homogeneous solution $P_0^{[\mathrm{I}]}(\eta, T)$, between the ord$(\epsilon^{-1})$ and ord(1) terms in the perturbation expansion (27).

Eq. (33) reveals two sources of asymmetry in the boundary layer. One of these, which is proportional to the cumulative probability $A(T)$, persists through to the final steady state. The other, proportional to the *rate of arrival* of probability $A'(T)$, is a transient effect.

5. Inner–outer matching and complete PDF

To bridge between the outer and inner solutions, consider an intermediate (matching) regime within ord(1) distance of x^*, for which we define the coordinate

$$\zeta = x - x^* = \epsilon\eta < 0 \tag{37}$$

In this vicinity the Smoluchowski Eq. (2) becomes

$$\epsilon\frac{\partial P^{[\mathrm{M}]}}{\partial t} + \frac{\partial}{\partial\zeta}\left\{\left[-4\gamma^2\zeta + O(\epsilon\zeta)\right]P^{[\mathrm{M}]} - \frac{\epsilon^2}{2}\frac{\partial P^{[\mathrm{M}]}}{\partial\zeta}\right\} = 0 \tag{38}$$

Again the ϵ factor multiplying the time derivative suggests a separation of timescales. But now—in contrast with the case for the inner solution—advection dominates over diffusion. Skipping details of the two-timescale analysis, we find the leading-order flux:

$$\left[-4\gamma^2\zeta + O(\epsilon\zeta)\right]P^{[\mathrm{M}]} \sim \text{Constant} = \epsilon A'(T) \tag{39}$$

Thus

$$P^{[\mathrm{M}]} \sim -\frac{A'(T)}{4\gamma^2}\left(\frac{\epsilon}{\zeta}\right) = -\frac{A'(T)}{4\gamma^2\eta} \quad \text{as } \zeta \nearrow 0 \tag{40}$$

This functional form constitutes the inner limiting behavior of the outer solution, and it is consistent with the outer limiting behavior of the inner solution, as given by Eqs. (33) and (35). Therefore we were justified in extending the inner solution into the outer domain in setting the normalization condition (36) on $P_1^{[\mathrm{I}]}$.

In view of the above discussion of matching, the asymptotic PDF over the whole domain can be obtained simply by adding the inner and outer solutions, as given by Eqs. (14), (17), (31) and (33):

$$P(x, t; \epsilon) \sim P_0^{[\mathrm{O}]}(x, t; \epsilon) + \epsilon^2 P_2^{[\mathrm{O}]}(x, t; \epsilon) + \epsilon^{-1}P_0^{[\mathrm{I}]}\left[\epsilon^{-1}(x - x^*), t\right] + P_1^{[\mathrm{I}]}\left[\epsilon^{-1}(x - x^*), t\right] \tag{41}$$

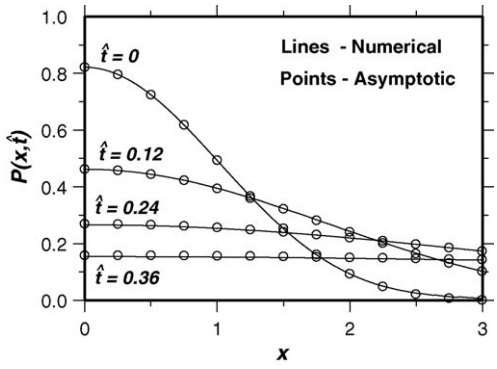

Fig. 2. Asymptotic vs. numerical PDFs plotted in the outer region for $\epsilon = 0.2$, $\gamma = 1$ ($L = 5$, $\Gamma = 5$).

Figs. 2 and 3 show good agreement between this formula and the corresponding numerical PDFs for $\epsilon = 0.2$ and $\gamma = 1$. The latter curves were calculated here using an atomistic smoothed particle hydrodyamics (ASPH) method [14,15,30], although a stochastic simulation [10,17] could also have been employed.

6. Stress buildup

Using the asymptotic PDF (41) for $\epsilon = 0.2$ and $\gamma = 1$ in the second moment equation and the Kramers integral for the stress [2,8,10–12,21],

$$\left\langle x^2 \right\rangle = \int_0^{\epsilon^{-1}} P(x,t)x^2 \, \mathrm{d}x \tag{42}$$

$$\tau(t) = \int_0^{\epsilon^{-1}} P(x,t)\frac{x^2}{1-\epsilon^2 x^2} \, \mathrm{d}x - 1 \tag{43}$$

we obtain (by numerical quadrature) stress buildup and stress–extension curves that are seen in Figs. 4 and 5 to compare favorably with the corresponding numerical curves. The discrepancy between the asymptotic versus numerical terminal, steady-state stresses in Fig. 4 can be traced to the order ϵ correction in the inner PDF, which is not included in Eq. (41).

One particularly interesting conclusion follows immediately from the dominance of the boundary-layer contribution in both the integrals (42) and (43).

$$\langle x^2 \rangle \sim A(t)\epsilon^{-2} = A(t)L^2 \tag{44}$$

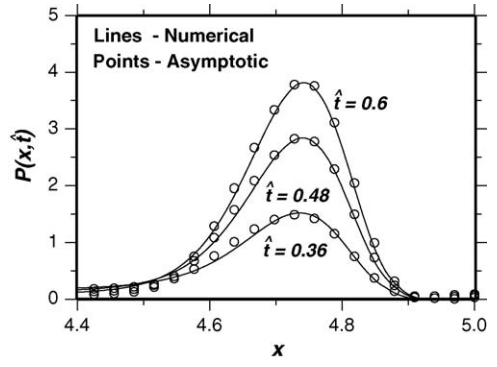

Fig. 3. Asymptotic vs. numerical PDFs plotted in the inner region for $\epsilon = 0.2$, $\gamma = 1$ ($L = 5$, $\Gamma = 5$).

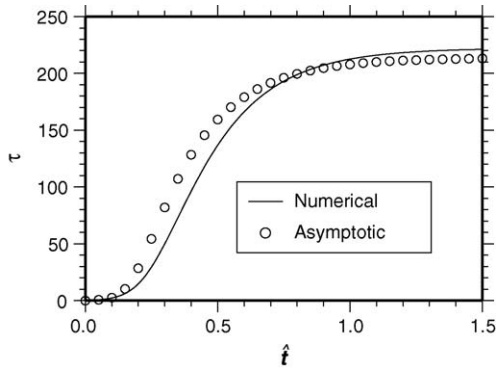

Fig. 4. Asymptotic vs. numerical stress buildup curves for stretching of a FENE dumbbell in a suddenly started uniaxial extensional flow. Here $\epsilon = 0.2$ and $\gamma = 1$ ($L = 5$, $\Gamma = 5$).

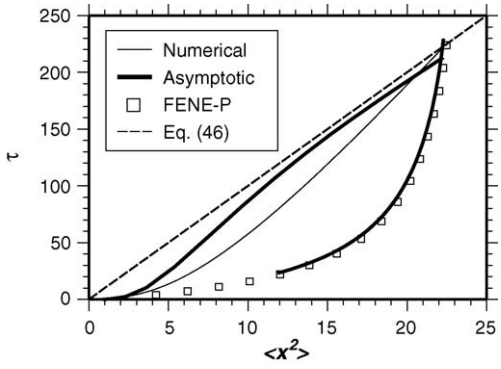

Fig. 5. Asymptotic vs. numerical stress–extension curves for elongation followed by relaxation. Here $\epsilon = 0.2$ and $\gamma = 1$ ($L = 5$, $\Gamma = 5$).

$$\tau(t) \sim A(t)2\gamma\epsilon^{-3} = A(t)2\Gamma L^2 \tag{45}$$

In the stress–extension plane we find a simple proportionality at leading order:

$$\tau \sim 2\Gamma\langle x^2 \rangle \tag{46}$$

For a fixed (large) value of Γ (Weissenberg number), the lines for different (sufficiently large) finite extensibility parameters L^2 should all collapse together. This result explains the analogous numerical observation by Doyle et al. [6] with regard to transient stress-birefringence curves, and—for large Weissenberg number—agrees with the large-strain plateau in the transient stress-optic coefficient, as described by Sizaire et al. [21]. Eq. (46) is shown as a dashed line in Fig. 5, and gives a rough but useful indication of FENE stretching behavior even at ϵ as large as 0.2.

7. Stress relaxation

The inner and outer solutions derived above hinge critically on (i) the detailed asymptotic structure and scaling of the advective and diffusive terms in the Smoluchowski equation in each regime, and (ii) the initial condition. Thus, a generic functional form for the PDF—applicable to arbitrary strain histories and/or strain-relaxation cycles—remains elusive. However, a particular case allows analytical progress on the problem of memory

effects in the rheology of dilute polymer solutions: relaxation of the PDF from the final steady-state in elongation, once all of the probability has accumulated in the boundary layer. Here we must omit the Γ term from the Smoluchowski Eq. (1).

$$\frac{\partial P}{\partial \hat{t}} - \frac{\partial}{\partial x}\left\{\left(\frac{x/2}{1-\epsilon^2 x^2}\right)P + \frac{1}{2}\frac{\partial P}{\partial x}\right\} = 0, \quad 0 < x < \epsilon^{-1} \tag{47}$$

$$P(x,0) = \left\{\int_0^{\epsilon^{-1}} \mathrm{e}^{(\gamma/\epsilon)x^2}(1-\epsilon^2x^2)^{1/(2\epsilon^2)}\,\mathrm{d}x\right\}^{-1} \times \mathrm{e}^{(\gamma/\epsilon)x^2}(1-\epsilon^2x^2)^{1/(2\epsilon^2)} \tag{48}$$

For short times, before the PDF has retracted far from its fully stretched configuration (48), we use the boundary layer coordinate η from Eq. (22), and a time variable

$$s = \epsilon^{-3}\hat{t} = \epsilon^{-2}t = \epsilon^{-1}\tau \tag{49}$$

that is one order faster than the *fast* time variable τ from Eq. (28).

$$\frac{\partial P}{\partial s} = \frac{\partial}{\partial \eta}\left\{V(\eta;\epsilon)P + \frac{\epsilon}{2}\frac{\partial P}{\partial \eta}\right\} \tag{50}$$

with

$$V(\eta;\epsilon) = \frac{\epsilon}{2}\left[\frac{\sqrt{1-\epsilon/(2\gamma)}+\epsilon^2\eta}{1-\left(\sqrt{1-\epsilon/(2\gamma)}+\epsilon^2\eta\right)^2}\right] \tag{51}$$

$$V(\eta;\epsilon) \sim \gamma\left[\frac{1-\epsilon/(4\gamma)+O(\epsilon^2)}{1-4\gamma\epsilon\eta+O(\epsilon^2)}\right] \tag{52}$$

The roughly Gaussian shape of the initial PDF (48) emerges upon writing it as a function the inner variable η.

$$\begin{aligned} P(\eta,0) = {} & \left(\frac{2\gamma}{\sqrt{\pi}}\right)\mathrm{e}^{-(2\gamma\eta)^2} \\ & + \frac{\epsilon}{\sqrt{\pi}}\left[(2\gamma\eta)^2 - \frac{8\gamma}{3}(2\gamma\eta)^3 - \frac{1}{2}\right]\mathrm{e}^{-(2\gamma\eta)^2} \\ & + \frac{\epsilon^2}{\sqrt{\pi}}\left[\frac{16\gamma}{9}(2\gamma\eta)^6 - \frac{4}{3}(2\gamma\eta)^5\right. \\ & + \left(\frac{1}{4\gamma} - 4\gamma\right)(2\gamma\eta)^4 + \frac{5}{3}(2\gamma\eta)^3 \\ & \left. - \frac{1}{4\gamma}(2\gamma\eta)^2 - \frac{1}{16\gamma} - \frac{\gamma}{3}\right]\mathrm{e}^{-(2\gamma\eta)^2} + O(\epsilon^3) \end{aligned} \tag{53}$$

This asymptotic expansion comes from applying a regular perturbation in ϵ to the steady-state version of the Smoluchowski Eq. (23), using the ascending velocity coefficients (24)–(26). Inserting the PDF (53) into the moment formula

$$M_k(s) = \langle \eta^k \rangle^{[\mathrm{I}]} = \int_{-\infty}^{\infty} \eta^k P(\eta, s)\,\mathrm{d}s \tag{54}$$

we find the initial values of the first two moments:

$$M_1(0) = \frac{-\epsilon}{2\gamma}\left[1 + \epsilon\left(\frac{5}{8\gamma}\right) + \cdots\right] \tag{55}$$

$$M_2(0) = \frac{1}{8\gamma^2}\left[1 + \epsilon\left(\frac{1}{2\gamma}\right) + \epsilon^2\left(4 + \frac{1}{4\gamma^2}\right) + \cdots\right] \tag{56}$$

From a numerical solution (not shown here) of the inner Smoluchowski Eq. (50), the PDF appears to become even more closely Gaussian as it retracts and broadens with advancing time s. Thus we are motivated to approximate $P(\eta, s)$ with the two-parameter Gaussian function

$$\mathcal{P}(\eta, s) = [2\pi\mathcal{M}(s)]^{-1/2}\exp\left\{-\frac{[\eta - \mathcal{C}(s)]^2}{2\mathcal{M}(s)}\right\} \tag{57}$$

Here $\mathcal{C}(s)$ is the location of the center of the peak (first moment), and $\mathcal{M}(s)$ is the peak-centered second moment,

$$\mathcal{M}(s) = \int_{-\infty}^{\infty}[\eta - \mathcal{C}(s)]^2\mathcal{P}(\eta, s)\,\mathrm{d}s \tag{58}$$

It is expedient to track $\mathcal{C}(s)$ with the advective velocity $V[\mathcal{C}(s);\epsilon]$ right at this (moving) point. The truncated velocity formula (52) then yields an ODE

$$\frac{\mathrm{d}\mathcal{C}}{\mathrm{d}s} = -\frac{\gamma - \epsilon/4}{1 - 4\gamma\epsilon\mathcal{C}(s)}, \quad \mathcal{C}(0) = M_1(0) \tag{59}$$

that can readily be solved:

$$\mathcal{C}(s) = \frac{1}{4\gamma\epsilon}\left[1 - \sqrt{As + B}\right] \tag{60}$$

with

$$A = 8\gamma^2\epsilon - 2\gamma\epsilon^2 \tag{61}$$

$$B = \left(1 + 2\epsilon^2 + \frac{5\epsilon^3}{4\gamma}\right)^2 \tag{62}$$

What we have done is tantamount to concentrating the (already narrow) PDF into a delta function, and this well-known argument is one way of viewing the Peterlin closure [6,11–13,24].

Our main purpose in this section is to go a step further, and estimate the time-varying width—equivalently, $\mathcal{M}(s)$—of the approximate Gaussian peak $\mathcal{P}(\eta, s)$. To this end, we shall, at each time s, impose the Smoluchowski Eq. (50) upon the Gaussian form (57) at only one special point: $\eta = \mathcal{C}(s)$. This crude "collocation" scheme,

$$\left.\frac{\partial \mathcal{P}}{\partial s}\right|_{\eta=\mathcal{C}(s)} = V'[\mathcal{C}(s)]\mathcal{P}[\mathcal{C}(s), s] + \frac{\epsilon}{2}\left[\frac{\partial^2\mathcal{P}}{\partial\eta^2}\right]_{\eta=\mathcal{C}(s)} \tag{63}$$

leads to an ODE for $\mathcal{M}(s)$:

$$\frac{\mathrm{d}\mathcal{M}}{\mathrm{d}s} = \epsilon - 2V'[\mathcal{C}(s)]\mathcal{M}(s) = \epsilon - \left(\frac{A}{As + B}\right)\mathcal{M}(s) \tag{64}$$

which can also be solved analytically.

$$\mathcal{M}(s) = (As + B)^{-1}\left[B\mathcal{M}(0) + \epsilon\left(\frac{A}{2}s^2 + Bs\right)\right] \tag{65}$$

For the initial value we make use of Eqs. (55) and (56)

$$\mathcal{M}(0) = M_2(0) - [M_1(0)]^2 \tag{66}$$

To illuminate the operative physics, we note the following feature of the Gaussian shape (57):

$$\mathcal{P}[\mathcal{C}(s), s] = -\mathcal{M}(s)\left[\frac{\partial^2 \mathcal{P}}{\partial \eta^2}\right]_{\eta=\mathcal{C}(s)} \tag{67}$$

Inserting this into the collocation Eq. (63), we find a form

$$\left.\frac{\partial \mathcal{P}}{\partial s}\right|_{\eta=\mathcal{C}(s)} = \left\{\frac{\epsilon}{2} - \mathcal{M}(s)V'[\mathcal{C}(s)]\right\}\left[\frac{\partial^2 \mathcal{P}}{\partial \eta^2}\right]_{\eta=\mathcal{C}(s)} = D_{\text{eff}}\left[\frac{\partial^2 \mathcal{P}}{\partial \eta^2}\right]_{\eta=\mathcal{C}(s)} \tag{68}$$

that looks like a diffusion equation, wherein the slope of the advective velocity reduces the effective diffusion coefficient D_{eff}. On reflection, this behavior is not surprising, because the decrease in velocity in the direction of the peak's motion has the effect of gathering probability together and thereby narrowing the peak, against the dispersing influence of diffusion. The standard definition of the diffusion coefficient in terms of the rate of growth of the second moment,

$$\frac{\mathrm{d}\mathcal{M}}{\mathrm{d}s} = 2D_{\text{eff}}s \tag{69}$$

leads precisely back to the ODE (64).

The above arguments are summarized in the following operational procedure. To obtain the transient PDF $P(x, \hat{t})$ for relaxation of the FENE dumbbell from its fully stretched configuration, one should insert

$$\eta = \epsilon^{-1}\left[x - \epsilon^{-1}\sqrt{1 - \frac{\epsilon}{2\gamma}}\right] \quad \text{and} \quad s = \epsilon^{-3}\hat{t} \tag{70}$$

into the Gaussian formula (57), where the time evolution of the coefficients $\mathcal{C}(s)$ and $\mathcal{M}(s)$ is given by Eqs. (60) and (65). For $\epsilon = 0.2$ and $\gamma = 1$, Fig. 6 compares a full numerical solution of the Smoluchowski equation (47) and (48) with our Gaussian approximation. Excellent agreement is observed. The corresponding stress decay curve is shown in Fig. 7, and the stress–extension curve appears in Fig. 5.

It is worth noting that—for stress relaxation—the Peterlin closure (which assumes a delta function spike for the PDF instead of the broadening peak) yields stress decay and stress extension curves that are almost indistinguishable from the numerics [11,12,24]. Thus, finite (and increasing) width of the PDF seems to have no important consequence for the rheology of stress relaxation.

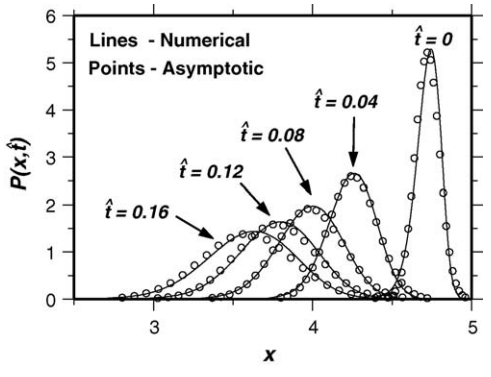

Fig. 6. Asymptotic vs. numerical PDFs for stress relaxation from the terminal steady state in uniaxial extension for $\epsilon = 0.2$, $\gamma = 1$ ($L = 5$, $\Gamma = 5$).

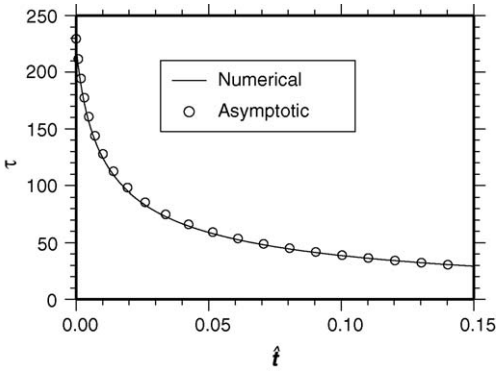

Fig. 7. Decay of the stress during relaxation from the final steady state in uniaxial extension for $\epsilon = 0.2$ and $\gamma = 1$. Numerical results are compared with the Gaussian approximation (57), (60) and (65). The Peterlin closure (FENE-P) is not plotted, as it would also be almost indistinguishable from the numerical curve.

8. Concluding remarks

Loops in the stress–extension plane are observed in transient elongation, because different PDFs in the stretching versus relaxing phases can be characterized by the same value of the second moment, while leading to different stresses [21,24,27,29]. At least a second-order closure, such as the L closure of Lielens et al. [11,12], is required to capture this memory effect. A one-parameter family of PDFs will necessarily lock the stress and extension together in a single-valued dependence. For example, the Peterlin closure yields a stress–extension curve that can only follow the relaxation portion of Fig. 5. For this regime it is very accurate.

For one special case of a strain-relaxation cycle, the asymptotic formulas derived in this paper gave a rigorous and detailed analytical representation of the underlying features of the PDFs that are responsible for memory effects, and also justified the L closure—which was originally motivated by numerical observations.

For stretching of a FENE dumbell in a uniaxial extensional flow, singular perturbation theory was combined with the method of multiple scales (Sections 1–5) to yield accurate formulas for the entire PDF, from which the stress buildup and stress–extension curves could then be calculated (Section 6). The leading-order asymptotics explained why the stress–extension curves for different finite-extensibility parameters should all collapse onto a single straight line, Eq. (46). This conclusion rigorously corroborated an analogous numerical observation by Doyle et al. [6] with regard to transient stress–birefringence curves, and—for large Weissenberg number—agreed with the large-strain plateau in the transient stress-optic coefficient, as described by Sizaire et al. [21]. The asymptotic stress–extension curve for stretching compared favorably with its numerical counterpart. The accuracy of this curve was roughly comparable to that of the L closure; cf. [[11], Fig. 14] and [[12], Fig. 10].

For relaxation of the FENE dumbbell from its fully stretched configuration, a Gaussian approximation of the PDF—whose time-dependent position and width were given by closed analytical formulas—matched the numerical results extremely well. The slope of the advective velocity was interpreted as a negative contribution to the effective diffusion coefficient.

A noteworthy feature of the asymptotics for both stretching and relaxation of the FENE dumbbell was their utility even when the perturbation parameter (inverse dumbbell length) was not very small ($\epsilon = 0.2$).

This paper illustrated the fruitful interplay between asymptotic theory and numerical analysis. The asymptotic approach employed here would not have traction in the absence of physical insight or of knowledge of the key features of the PDF—which for this problem were originally established by detailed stochastic simulations [5,6,8,10–12,17].

Acknowledgement

The author would like to thank Professor E.J. Hinch, DAMTP, University of Cambridge, UK, for a series of very helpful conversations during the early stages of this work.

References

[1] C.M. Bender, S.A. Orszag, Advanced Mathematical Methods for Scientists and Engineers, McGraw-Hill, New York, 1978.
[2] R.B. Bird, C.F. Curtiss, R.C. Armstrong, O. Hassager, Dynamics of Polymeric Liquids: Kinetic Theory, vol. 2, 2nd ed., Wiley-Interscience, New York, 1987.
[3] G.F. Carrier, C.E. Pearson, Partial Differential Equations: Theory and Technique, Academic Press, New York, 1976.
[4] P.G. De Gennes, Coil-stretch transition of dilute flexible polymer under ultrahigh velocity gradients, J. Chem. Phys. 60 (1974) 5030–5042.
[5] P.S. Doyle, E.S.G. Shaqfeh, Dynamic simulation of freely draining, flexible bead-rod chains: start-up of extensional and shear flow, J. Non-Newtonian Fluid Mech. 76 (1998) 43–78.
[6] P.S. Doyle, E.S.G. Shaqfeh, G.H. McKinley, S.H. Spiegelberg, Relaxation of dilute polymer solutions following extensional flow, J. Non-Newtonian Fluid Mech. 76 (1998) 79–110.
[7] I. Ghosh, G.H. McKinley, R.A. Brown, R.C. Armstrong, Defficiencies of FENE dumbbell models in describing the rapid stretching of dilute polymer solutions, J. Rheol. 45 (2001) 721–758.
[8] M. Herrchen, H.C. Öttinger, A detailed comparison of various FENE dumbbell models, J. Non-Newtonian Fluid Mech. 68 (1997) 17–42.
[9] E.J. Hinch, Mechanical models of dilute polymer solutions in strong flows, Phys. Fluids 20 (1977) S22–S30.
[10] R. Keunings, On the Peterlin approximation for finitely extensible dumbbells, J. Non-Newtonian Fluid Mech. 68 (1997) 85–100.
[11] G. Lielens, P. Halin, I. Jaumain, R. Keunings, V. Legat, New closure approximations for the kinetic theory of finitely extensible dumbbells, J. Non-Newtonian Fluid Mech. 76 (1998) 249–279.
[12] G. Lielens, R. Keunings, V. Legat, The FENE-L and FENE-LS closure approximations to the kinetic theory of finitely extensible dumbbells, J. Non-Newtonian Fluid Mech. 87 (1999) 179–196.
[13] G.H. McKinley,. Extensional rheology and flow instabilities in elastic polymer solutions dynamics of complex fluids, in: M.J. Adams (Ed.), Proceedings of the Royal Society, Unilever Indo, UK Forums, vol. 1, J. Imperial College Press, London, 1997.
[14] L.C. Nitsche, W. Zhang, Atomistic SPH and a link between diffusion and interfacial tension, AIChE J. 48 (2002) 201–211.
[15] L.C. Nitsche, W. Zhang, L.E. Wedgewood, Asymptotic basis of the L closure for finitely extensible dumbbells in suddenly started uniaxial extension, J. Non-Newtonian Fluid Mech. 133 (2006) 14–27.
[16] H.C. Öttinger, A model of dilute polymer solutions with hydrodynamic interaction and finite extensibility. I. Basic equations and series expansions, J. Non-Newtonian Fluid Mech. 26 (1987) 207–246.
[17] H.C. Öttinger, Stochastic Processes in Polymeric Fluids, 1st ed., Springer, Berlin, 1996.
[18] A. Peterlin, Hydrodynamics of macromolecules in a velocity field with longitudinal gradient, J. Polym. Sci.: Polym. Lett. 4B (1966) 287–291.
[19] J.M. Rallison, E.J. Hinch, Do we understand the physics in the constitutive equation?, J. Non-Newtonian Fluid Mech. 29 (1988) 37–55.
[20] P. Singh, L.G. Leal, Computational studies of the FENE dumbbell model with conformation-dependent friction in a co-rotating two-roll mill, J. Non-Newtonian Fluid Mech. 67 (1996) 137–178.
[21] R. Sizaire, G. Lielens, I. Jaumain, R. Keunings, V. Legat, On the hysteretic behaviour of dilute polymer solutions in relaxation following extensional flow, J. Non-Newtonian Fluid Mech. 82 (1999) 233–253.
[22] A.J. Szeri, A deformation tensor model for nonlinear rheology of FENE polymer solutions, J. Non-Newtonian Fluid Mech. 92 (2000) 1–25.
[23] R.I. Tanner, Stresses in dilute solutions of bead-nonlinear-spring macromolecules. III. Friction coefficient varying with dumbbell extension, Trans. Soc. Rheol. 19 (1975) 557–582.
[24] R.I. Tanner, Engineering Rheology, 2nd ed., Oxford University Press, New York, 2000.
[25] H.R. Warner, Kinetic theory and rheology of dilute suspensions of finitely extendible dumbbells, Ind. Eng. Chem. Fundm. 11 (1972) 379–387.
[26] L.E. Wedgewood, A Gaussian closure of the second-moment equation for a Hookean dumbbell with hydrodynamic interaction, J. Non-Newtonian Fluid Mech. 31 (1989) 127–142.
[27] L.E. Wedgewood, R.B. Bird, From molecular models to the solution of flow problems, Ind. Eng. Chem. Res. 27 (1988) 1313–1320.
[28] L.E. Wedgewood, H.C. Öttinger, A model of dilute polymer solutions with hydrodynamic interaction and finite extensibility. II. Shear flows, J. Non-Newtonian Fluid Mech. 27 (1988) 245–264.
[29] J.M. Wiest, L.E. Wedgewood, R.B. Bird, On coil-stretch transitions in dilute polymer solutions, J. Chem. Phys. 90 (1989) 587–594.
[30] W. Zhang. Particle Methods and Perturbation Theory in Transport Phenomena: Polymer Rheology and Membrane Separations, Ph.D. Thesis, University of Illinois, Chicago, 2004.
[31] Q. Zhou, R. Akhavan, Cost-effective multi-mode FENE bead-spring models for dilute polymer solutions, J. Non-Newtonian Fluid Mech. 116 (2004) 269–300.
[32] W. Zylka, H.C. Öttinger, A comparison between simulations and various approximations for Hookean dumbbells with hydrodyamic interaction, J. Chem. Phys. 90 (1989) 474–480.